

## Quantum Critical Transport near the Mott Transition

H. Terletska,<sup>1</sup> J. Vučićević,<sup>2</sup> D. Tanasković,<sup>2</sup> and V. Dobrosavljević<sup>1</sup>

<sup>1</sup>Department of Physics and National High Magnetic Field Laboratory, Florida State University, Tallahassee, Florida 32306, USA

<sup>2</sup>Scientific Computing Laboratory, Institute of Physics Belgrade, University of Belgrade, Pregrevica 118, 11080 Belgrade, Serbia

(Received 26 January 2011; published 5 July 2011)

We perform a systematic study of incoherent transport in the high temperature crossover region of the half filled one-band Hubbard model. We demonstrate that the family of resistivity curves displays characteristic quantum critical scaling of the form  $\rho(T, \delta U) = \rho_c(T)f(T/T_0(\delta U))$ , with  $T_0(\delta U) \sim |\delta U|^{z\nu}$ , and  $\rho_c(T) \sim T$ . The corresponding  $\beta$  function displays a “strong coupling” form  $\beta \sim \ln(\rho_c/\rho)$ , reflecting the peculiar mirror symmetry of the scaling curves. This behavior, which is surprisingly similar to some experimental findings, indicates that Mott quantum criticality may be acting as the fundamental mechanism behind the unusual transport phenomena in many systems near the metal-insulator transition.

DOI: 10.1103/PhysRevLett.107.026401

PACS numbers: 71.27.+a, 71.30.+h

Many systems close to the metal-insulator transition (MIT) often display surprisingly similar transport features in the high temperature regime [1–3]. Here, the family of resistivity curves typically assumes a characteristic “fan-shaped” form [see Fig. 1(a)], reflecting a gradual crossover from metallic to insulating transport. At the highest temperatures the resistivity depends only weakly on the control parameter (concentration of charge carriers [1] or pressure [2,3]), while as  $T$  is lowered, the system seems to “make up its mind” and rapidly converges towards either a metallic or an insulating state. Since temperature acts as a natural cutoff scale for the metal-insulator transition, such behavior is precisely what one expects for quantum criticality [4]. In some cases [1], the entire family of curves displays beautiful scaling behavior, with a remarkable “mirror symmetry” of the relevant scaling functions [4]. But under which microscopic conditions should one expect such scaling phenomenology? What is the corresponding driving force for the transitions? Despite recent progress, such basic physics questions remain the subject of much ongoing controversy and debate.

The phenomenon of disordered-driven Anderson localization of noninteracting electrons is at present rather well understood based on the scaling formulation [5] and is generally viewed as an example of a  $T = 0$  quantum phase transition. On the other hand, a considerable number of recent experiments [1] provide compelling evidence that strong correlation effects—some form of Mott localization—may be the dominant mechanism [6]. Should one expect similar or very different transport phenomenology in the Mott picture? Is the paradigm of quantum criticality even a useful language to describe high temperature transport around the Mott point? These issues are notoriously difficult to address, because conventional Fermi liquid concepts simply cannot be utilized in the relevant high temperature incoherent regime. In this Letter, we answer this question in the framework

of dynamical mean-field theory (DMFT) [7], the only theoretical method that is most reliable precisely at high temperatures.

*Model and DMFT solution.*—We consider a single-band Hubbard model at half filling

$$H = - \sum_{\langle i,j \rangle \sigma} t_{ij}(c_{i\sigma}^\dagger c_{j\sigma} + \text{c.c.}) + \sum_i U n_{i\uparrow} n_{i\downarrow}, \quad (1)$$

where  $c_{i\sigma}^\dagger$  and  $c_{i\sigma}$  are the electron creation and annihilation operators, respectively,  $n_{i\sigma} = c_{i\sigma}^\dagger c_{i\sigma}$ ,  $t_{ij}$  is the hopping amplitude, and  $U$  is the repulsion between two electrons on the same site. We use a semicircular density of states, and the corresponding half-bandwidth  $D$  is set to be our energy unit. We focus on the paramagnetic DMFT

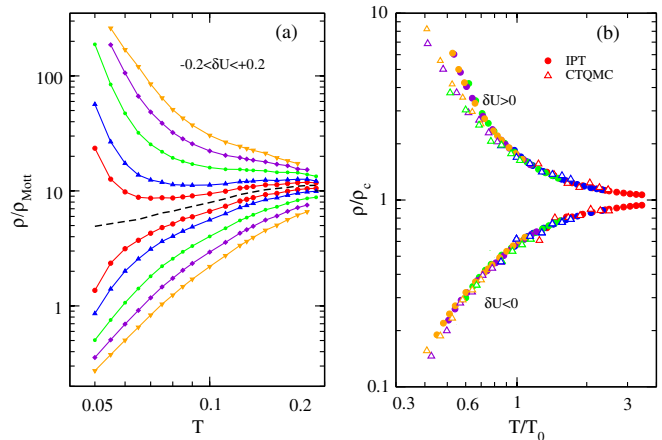


FIG. 1 (color online). (a) DMFT resistivity curves as a function of temperature along different trajectories  $-0.2 \leq \delta U \leq +0.2$  with respect to the instability line  $\delta U = 0$  (black dashed line; see the text). Data are obtained by using IPT impurity solver. (b) Resistivity scaling; essentially identical scaling functions are found from CTQMC (open symbols) and from IPT (closed symbols).

solution, which is formally exact in the limit of large coordination. Here the Hubbard model maps onto an effective Anderson impurity model supplemented by a self-consistency condition [7]. To solve the DMFT equations we use the iterated perturbation theory (IPT) [7] and cross-check our results with numerically exact continuous time quantum Monte Carlo (CTQMC) calculations [8,9]. We find, in agreement with previous work [10], that after appropriate energy rescaling (see below), the two methods produce qualitatively and even quantitatively identical results in the incoherent crossover region that we examine.

It is well known that at very low temperatures  $T < T_c \sim 0.03$ , this model features a first-order metal-insulator transition terminating at the critical end point  $T_c$  (Fig. 2), very similar to the familiar liquid-gas transition [10]. For  $T > T_c$ , however, different crossover regimes have been tentatively identified [7,11], but they have not been studied in any appreciable detail. The fact that the first-order coexistence region is restricted to such very low temperatures provides strong motivation to examine the high temperature crossover region from the perspective of “hidden quantum criticality.” In other words, the presence of a coexistence dome at  $T < T_c \ll 1$ , an effect with a very small energy scale, is not likely to influence the behavior at much higher temperatures  $T \gg T_c$ . In this high temperature regime smooth crossover is found, which may display behavior consistent with the presence of a “hidden” quantum critical (QC) point at  $T = 0$ . To test this idea, we utilize standard scaling methods appropriate for quantum

criticality and compute the resistivity curves along judiciously chosen trajectories respecting the symmetries of the problem.

*Instability trajectory formalism.*—Previous work has already recognized [10] that, in order to reveal the proper scaling behavior close to the critical end point, one has to follow a set of trajectories parallel to “zero field” trajectory  $U^*(T)$ . We thus expect  $\delta U \equiv U - U^*(T)$  to play the role of the scaling variable corresponding to a symmetry-breaking field favoring one of the two competing (metal vs insulator) phases. By analogy [10,12] to the familiar liquid-gas transition, we determine the precise location of such an “instability trajectory” by examining the curvature of the corresponding free energy functional [13]. This curvature vanishes at  $T_c$  and is finite and minimal at  $T > T_c$ , along this instability line. Consequently, as in Refs. [10,13,14], our problem is recast as an eigenvalue analysis of the corresponding free energy functional  $\mathcal{F}[G(i\omega_n)]$  for which the DMFT Green’s function solution  $G_{\text{DMFT}}(i\omega_n)$  represents a local extremum and can be regarded as a vector in an appropriate Hilbert space.

The free energy near such an extremum can be written as  $\mathcal{F}[G(i\omega_n)] = \mathcal{F}_0 + Tt^2 \sum_{m,n} \delta G(i\omega_m) M_{mn} \delta G(i\omega_n) + \dots$ , where

$$M_{mn} = \frac{1}{2Tt^2} \left. \frac{\partial^2 \mathcal{F}[G]}{\partial G(i\omega_m) \partial G(i\omega_n)} \right|_{G=G_{\text{DMFT}}} \quad (2)$$

and  $\delta G(i\omega_n) \equiv G(i\omega_n) - G_{\text{DMFT}}(i\omega_n)$ . The curvature of the free energy functional is determined by the lowest eigenvalue  $\lambda$  of the fluctuation matrix  $M$ . As explained in Ref. [15],  $\lambda$  can be obtained from the iterative solution of DMFT equations. The difference of the Green’s functions in iterations  $n$  and  $n + 1$  of the DMFT self-consistency loop is given by

$$\delta G^{(n+1)}(i\omega_n) - \delta G^{(n)}(i\omega_n) = e^{-n\lambda} \delta G^{(0)}(i\omega_n), \quad (3)$$

and therefore  $\lambda$  determines the rate of convergence of the Green function to its solution.

An example of our calculations is shown in the inset in Fig. 2, where the eigenvalues at several temperatures are plotted as a function of interaction  $U/U_c$ . The minima of these curves define the locus of the instability trajectory  $U^*(T)$ , which terminates at the critical end point  $(U_c, T_c)$ , as shown in Fig. 2. Note that the immediate vicinity  $T \approx T_c$  of the critical end point has been carefully studied theoretically [10] and even observed in experiments [2], revealing classical Ising scaling (since one has a finite temperature critical point) of transport in this regime. In our study, we examine the crossover behavior at much higher temperatures  $T \gg T_c$ , displaying very different behavior: precisely what is expected in presence of quantum criticality.

*Resistivity calculation.*—To reveal quantum critical scaling, we calculate the temperature dependence of the resistivity along a set of trajectories parallel to our instability trajectory [fixed  $\delta U = U - U^*(T)$ ]. Resistivity was calculated by using standard DMFT procedures [7], with

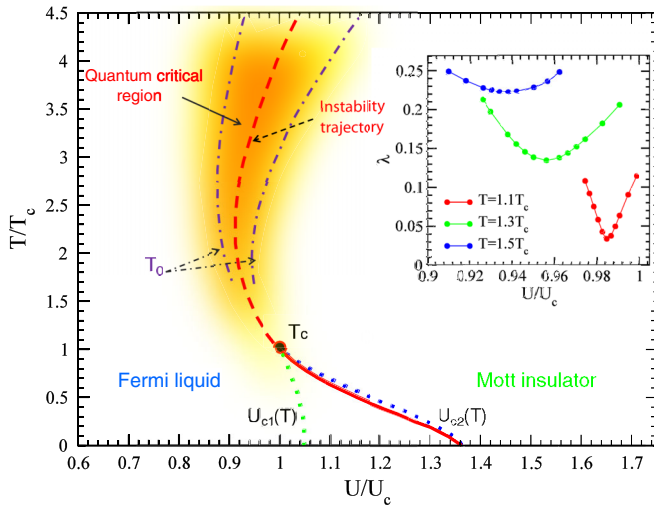


FIG. 2 (color online). DMFT phase diagram of the fully frustrated half filled Hubbard model, with a shaded region showing where quantum critical-like scaling is found. Metallic  $U_{c2}(T)$  and insulating  $U_{c1}(T)$  spinodals (dotted lines) are found at  $T < T_c$ ; the corresponding first-order phase transition is shown by a thick solid line. The thick dashed line, which extends at  $T > T_c$ , shows the instability trajectory  $U^*(T)$ , and the crossover temperature  $T_0$  delimits the QC region (dash-dotted lines). The inset shows examples of eigenvalue curves at three different temperatures, with pronounced minima at  $U^*(T)$  determining the instability trajectory.

the maximum entropy method [16] utilized to analytically continue CTQMC data to the real axis. The resistivity results are shown in Fig. 1, where in panel (a) IPT resistivity data for  $\delta U = 0, \pm 0.025, \pm 0.05, \pm 0.1, \pm 0.15, \pm 0.2$  in the temperature range of  $T \approx 0.07\text{--}0.2$  are presented (CTQMC data are not shown for the sake of clarity of the figure). The resistivity is given in units of  $\rho_{\text{Mott}}$ , maximal resistivity according to the Boltzmann quasiclassical theory of transport [17]. The family of resistivity curves above ( $\delta U > 0$ ) the “separatrix”  $\rho_c(T)$  (dashed line, corresponding to  $\delta U = 0$ ) has an insulatinglike behavior, while metallic dependence is obtained for  $\delta U < 0$ .

*Scaling analysis.*—According to what is generally expected for quantum criticality, our family of curves should satisfy the following scaling relation:

$$\rho(T, \delta U) = \rho_c(T)f(T/T_0(\delta U)). \quad (4)$$

We thus first divide each resistivity curve by the separatrix  $\rho_c(T) = \rho(T, \delta U = 0)$  and then rescale the temperature, for each curve, with an appropriately chosen parameter  $T_0(\delta U)$  to collapse our data onto two branches [Fig. 1(b)]. Note that this unbiased analysis does not assume any specific form of  $T_0(\delta U)$ : It is determined for each curve simply to obtain optimum collapse of the data [18]. This puts us in a position to perform a stringent test of our scaling hypothesis: True quantum criticality corresponds to  $T_0(\delta U)$ , which vanishes at  $\delta U = 0$  and displays power-law scaling with the same exponents for both scaling branches. As seen in Fig. 3(a),  $T_0$  falls sharply as  $U = U^*$  is approached, consistent with the QC scenario but opposite to what is expected in a “classical” phase transition. The inset in Fig. 3(a) with log-log scale shows clearly a power-law behavior of  $T_0 = c|\delta U|^{z\nu}$ , with the estimated power  $(z\nu)_{\delta U < 0}^{\text{IPT}} = 0.56 \pm 0.01$  for the “metallic” side and  $(z\nu)_{\delta U > 0}^{\text{IPT}} = 0.57 \pm 0.01$  for an insulating branch.

We also find [Fig. 3(b)] a very unusual form of our critical resistivity  $\rho_c(T)$ , corresponding to the instability trajectory.

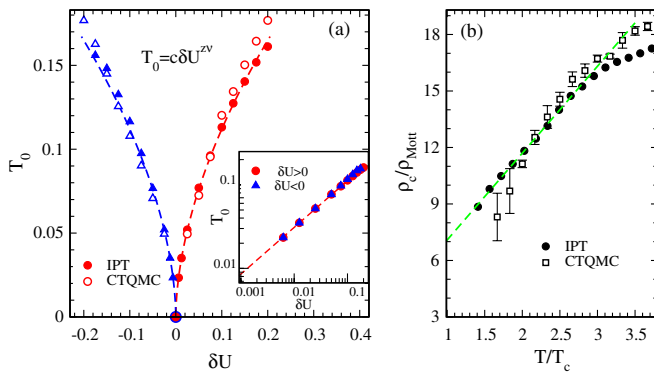


FIG. 3 (color online). (a) Scaling parameter  $T_0(\delta U)$  as a function of control parameter  $\delta U = U - U^*$ ; the inset illustrates power-law dependence of scaling parameter  $T_0 = c|\delta U|^{z\nu}$ . (b) Resistivity  $\rho_c(T)$  of the separatrix. Excellent agreement is found between IPT (closed symbols) and CTQMC (open symbols) results.

Its values largely exceeds the Mott limit, yet it displays metalliclike but non-Fermi liquidlike temperature dependence  $\rho_c(T) \sim T$ . Such puzzling behavior, while inconsistent with any conventional transport mechanism, has been observed in several strongly correlated materials close to the Mott transition [17,20]. Our results thus suggest that it represents a generic feature of Mott quantum criticality.

*$\beta$  function and mirror symmetry of scaled curves.*—To specify the scaling behavior even more precisely, we compute the corresponding  $\beta$  function [4]  $\beta(g) = \frac{d \ln g}{d \ln T}$ , with  $g = \rho_c/\rho$  being the inverse resistivity scaling function. Remarkably [Fig. 4(a)], it displays a nearly linear dependence on  $\ln g$  and is continuous through  $\delta U = 0$  indicating precisely the same form of the scaling function on both sides of the transition—another feature exactly of the form expected for genuine quantum criticality. This functional form is very natural for the insulating transport, as it is obtained even for simple activated behavior  $\rho(T) \sim e^{-E_g/T}$ . The fact that the same functional form persists well into the metallic side is a surprise, especially since it covers almost an order of magnitude for the resistivity ratio. Such a behavior has been interpreted [4] to reflect the “strong coupling” nature of the critical point, which presumably is governed by the same physical processes that dominate the insulator. This points to the fact that our QC behavior has a strong coupling, i.e., nonperturbative character.

The fact that the  $\beta$  function assumes this logarithmic form on both sides of the transition is mathematically equivalent [4] to stating that the two branches of the corresponding scaling functions display “mirror symmetry” over the same resistivity range. Indeed, we find that transport in this QC region exhibits a surprisingly developed reflection symmetry [dashed vertical lines of Fig. 4(a) mark its boundaries]. Such a symmetry is clearly seen in Fig. 4(b), where the resistivity  $\rho/\rho_c$  (for  $\delta U > 0$ ) and conductivity  $\sigma/\sigma_c = \rho_c/\rho$  ( $\delta U < 0$ ) can be mapped onto each other by reflection with  $\frac{\rho(\delta U)}{\rho_c} = \frac{\sigma(-\delta U)}{\sigma_c}$  [21].

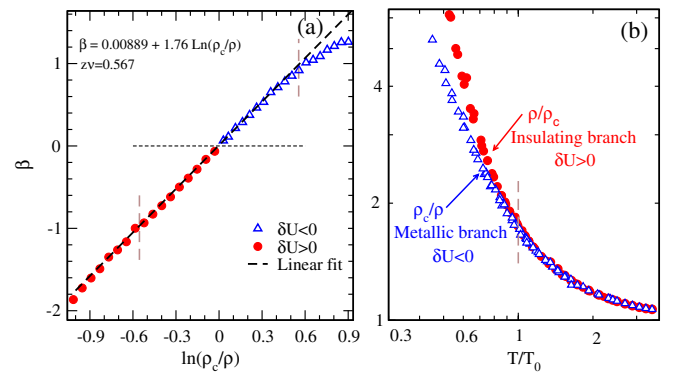


FIG. 4 (color online). (a) The  $\beta$  function shows linear in  $\ln(\rho_c/\rho)$  behavior close to the transition. Open symbols are for the metallic branch ( $\delta U < 0$ ), and closed ones are for the insulating side ( $\delta U > 0$ ); vertical dashed lines indicate the region where mirror symmetry of curves is found. (b) Reflection symmetry of scaled curves close to the transition.

Note that  $T/T_0 = 1$  sets the boundary of the quantum critical region, over which the reflection symmetry of scaled curves is observed. It is depicted by dash-dotted crossover lines  $T_0$  in the phase diagram of Fig. 2 [15].

These remarkable features of the  $\beta$  function, and associated reflection symmetry, have been observed earlier in experimental [1,21] and theoretical [4] studies, which tentatively associated this with disorder-dominated MITs. Speculation that  $\beta \sim \ln g$  reveals disorder as the fundamental driving force for MIT presumably reflects the fact that, historically, it has first been recognized for Anderson transitions [5]. Our work, however, shows that such behavior can be found even in the absence of disorder—in interaction-driven MITs. This finding calls for rethinking of basic physical processes that can drive the MIT.

*Conclusions.*—We have presented a careful and detailed study of incoherent transport in the high temperature crossover regime above the critical end point  $T_c$  of a single-band Hubbard model. Our analysis revealed a so-far overlooked scaling behavior of the resistivity curves, which we interpreted as evidence of hidden Mott quantum criticality. Precisely locating the proposed QC point in our model is hindered by presence of the low temperature coexistence dome, which limits our quantum critical scaling to the region well above  $T_c$ . Regarding the nature of transport in the QC regime, we found that the critical resistivity well exceeds the Mott limit, and yet it—surprisingly—assumes a metallic form, in dramatic contrast to conventional MIT scenarios. These features, together with large amounts of entropy characterizing this entire regime [22], prove surprisingly reminiscent of the “holographic duality” scenario [23,24] for a yet-unspecified QC point. Interestingly, the holographic duality picture has—so far—been discussed mostly in the context of quantum criticality in correlated metals (e.g.,  $T = 0$  magnetic transitions in heavy fermion compounds). Ours is the first work proposing that the same physical picture could apply to quantum criticality found at the MIT.

We believe that our results provide a significant new perspective on QC around the Mott transition and a deeper understanding of an apparent universality in the high temperature crossover regime. Our method traces a clear avenue for further searches for QC scaling, which are likely to be found in many other regimes and models.

In particular, it would be interesting to study a corresponding critical regime by going beyond the single-site DMFT analysis. It was shown in Ref. [19] that inclusion of spatial fluctuations does not significantly modify the high temperature crossover region in the half filled Hubbard model. Consequently, we expect our main findings to persist. An even more stringent test of our ideas should be provided in models where the critical end point  $T_c$  can be significantly reduced. This may include studies of the Mott transition away from half filling [25] or in systems with frustrations [6,26]. In such situations the proposed scaling regime should extend to much lower temperatures,

perhaps revealing more direct evidence of the—so far—hidden Mott QC point. Our ideas should also be tested by performing more detailed transport experiments in the relevant incoherent regime, a task that may be easily accessible in various organic Mott systems [3], where  $T_c$  is sufficiently below room temperature.

The authors thank K. Haule for the usage of his CTQMC code and M. Jarrell for the use of his maximum entropy code for analytical continuation of the CTQMC data. This work was supported by the National High Magnetic Field Laboratory and the NSF through Grants No. DMR-0542026 and No. DMR-1005751 (H.T. and V.D.) and Serbian Ministry of Science under Project No. ON171017 (J.V. and D.T.). D.T. acknowledges support from the NATO Science for Peace and Security Programme Grant No. EAP.RIG.983235. Numerical simulations were run on the AEGIS e-Infrastructure, supported in part by FP7 projects EGI-InSPIRE, PRACE-IIP, and HP-SEE.

- 
- [1] E. Abrahams *et al.*, *Rev. Mod. Phys.* **73**, 251 (2001).
  - [2] P. Limelette *et al.*, *Science* **302**, 89 (2003).
  - [3] F. Kagawa *et al.*, *Nature (London)* **436**, 534 (2005).
  - [4] V. Dobrosavljević *et al.*, *Phys. Rev. Lett.* **79**, 455 (1997).
  - [5] E. Abrahams *et al.*, *Phys. Rev. Lett.* **42**, 673 (1979).
  - [6] A. Camjayi *et al.*, *Nature Phys.* **4**, 932 (2008).
  - [7] A. Georges *et al.*, *Rev. Mod. Phys.* **68**, 13 (1996).
  - [8] P. Werner *et al.*, *Phys. Rev. Lett.* **97**, 076405 (2006).
  - [9] K. Haule, *Phys. Rev. B* **75**, 155113 (2007).
  - [10] G. Kotliar *et al.*, *Phys. Rev. Lett.* **84**, 5180 (2000).
  - [11] M. J. Rozenberg *et al.*, *Phys. Rev. Lett.* **75**, 105 (1995).
  - [12] J. H. Mooij, *Phys. Status Solidi A* **17**, 521 (1973).
  - [13] G. Moeller, V. Dobrosavljevic, and A. E. Ruckenstein, *Phys. Rev. B* **59**, 6846 (1999).
  - [14] M. J. Case and V. Dobrosavljević, *Phys. Rev. Lett.* **99**, 147204 (2007).
  - [15] See supplemental material at <http://link.aps.org/supplemental/10.1103/PhysRevLett.107.026401> for eigenvalue analysis and scaling procedure.
  - [16] M. Jarrell and J. E. Gubernatis, *Phys. Rep.* **269**, 133 (1996).
  - [17] N. E. Hussey *et al.*, *Philos. Mag.* **84**, 2847 (2004).
  - [18] Other criteria have also been employed to identify a MIT crossover line. Reference [19] used the flatness of the lowest Matsubara points of the self-energy; Refs. [7,11] used the inflection point of the resistivity curves. We have not reveal any apparent scaling behavior following these trajectories.
  - [19] H. Park, K. Haule, and G. Kotliar, *Phys. Rev. Lett.* **101**, 186403 (2008).
  - [20] B. J. Powell and R. H. McKenzie, *J. Phys. Condens. Matter* **18**, R827 (2006).
  - [21] D. Simonian, S. V. Kravchenko, and M. P. Sarachik, *Phys. Rev. B* **55**, R13 421 (1997).
  - [22] L. De Leo *et al.*, *Phys. Rev. A* **83**, 023606 (2011).
  - [23] S. Sachdev, *Phys. Rev. Lett.* **105**, 151602 (2010).
  - [24] J. McGreevy, *Physics* **3**, 83 (2010).
  - [25] G. Sordi, A. Amaricci, and M. J. Rozenberg, *Phys. Rev. B* **80**, 035129 (2009).
  - [26] M. Eckstein *et al.*, *Phys. Rev. B* **75**, 125103 (2007).